Mineral. Deposita 30, 11–19 (1995)

MINERALIUM DEPOSITA

Adularia in epithermal veins, Queensland: morphology, structural state and origin

G. Dong and G.W. Morrison*

Geology Department, James Cook University of North Queensland, Q4811, Australia

Received: 16 September 1993 / Accepted: 17 March 1994

Abstract. Four types of adularia (i.e. sub-rhombic, rhombic, tabular and pseudo-acicular) are recognised from examination of samples from ten epithermal vein deposits and prospects in Queensland, based on morphology of the individual crystals. Further investigation of the structural state of adularia reveals that each group has some specific features in terms of the degree of Al/Si disordering, which can be related to various crystallisation conditions and the thermal history. Sub-rhombic adularia is commonly 2–4 mm in size and subhedral with more or less rhombic outlines, and has a relatively ordered Al/Si distribution ($2t_1 > 0.84$), reflecting slow crystallisation conditions. Adularia of this type, in association with coarse-grained quartz, is predominant at deep levels of epithermal systems where boiling is initiated in an environment of low permeability and the fluid is slightly supersaturated with respect to adularia and quartz. Tabular adularia, characterised by its lath-shape and disordered structure ($2t_1$ values ranging from 0.64 to 0.74), is likely to have formed when the fluid moves up to a more permeable environment and starts boiling violently. Relatively high temperatures and rapidly changing conditions account for its special morphology and disordered structure. Rhombic adularia, showing very small crystal size (< 0.2 mm) with euhedral rhombic form, has an intermediate degree of Al/Si ordering. Pseudo-acicular adularia is interpreted as pseudomorphs after carbonate, and its high Al/Si ordered structure is attributed to the presence of a carbonate precursor. These two types of adularia commonly occur within crustiform and colloform bands in association with high grade ore, and chalcedony or fine-grained quartz which often displays various recrystallisation textures. It is most likely that adularias of these two types are formed when extensive boiling is protracted. Microprobe analyses indicate the composition of all adularia types close to pure $KAlSi_3O_8$. Sericite- and/or carbonate-altered adularias consistently display more ordered structures, suggesting that the post-crystallisation thermal regime affects the structural state of altered adularia, even at temperatures as low as in epithermal environments.

The term "adularia" is usually defined as a morphologically distinctive variety of potassium feldspar, typical of low-temperature hydrothermal environments (cf. Smith 1974; Černý and Chapman 1986). Studies of the optical and structural state of adularia from Alpine fissures and various hydrothermal veins have been conducted by a number of researchers (Gubser and Laves 1967; Colville and Ribbe 1968; Akizuki and Sunagawa 1978; Dimitriadis and Soldatos 1978; Černý and Chapman 1984 and 1986). These studies indicate that there is an extensive variability in the optical and structural state of adularia (ranging from maximum microcline to ideally disordered high sanidine), which may be related to variable kinetic conditions during crystallisation and the thermal regime after crystallisation.

In epithermal veins, adularia is well known as a distinctive gangue mineral. The presence of adularia is a critical distinction for two types of epithermal veins (adularia-sericite- and acid-sulphate-types) (Heald et al. 1987). Based on experiences in exploration of active geothermal systems, Browne (1978) suggested that the presence of vein adularia, formed due to the depositing fluid becoming more alkaline, is one of the indicators of boiling. Buchanan (1981) summarised data for over 60 epithermal vein deposits in western U.S. and found that the ore shoots typically contain significant amounts of adularia.

In the present study, the examination of samples from ten epithermal vein deposits in north and central Queensland suggests that there are some distinctive differences in the crystal form of adularia and the morphology of its crystal aggregates, and that only some types of adularia are associated with gold mineralisation. These findings have led to more detailed study of the structural state of adularia in these ten epithermal vein deposits, with regard to the usefulness of adularia as being an indicator of crystallisation conditions and thermal history.

* *Present address*: Klondike Exploration Services, 7 Mary Street, Townsville Q4810, Australia

Table 1. Geological information of studied epithermal vein deposits

Deposit	Tonnage (tons)	Production		Grade		Major hosts	Ore age
		Au (oz)	Ag (oz)	Au (g/t)	Ag (g/t)		
Golden Plateau	1,553,491 (underground)	595,686	672,000	12.2	13.5	Late Carboniferous to Lower Permian andesites	291.1 ± 5.3 (m.y.)
	1,028,946 (open pit)	146,124		4.4			
Dawn	1,369	868	2654	19.6	59.4	As above	
Central Extended	1,789 (underground)	589	135	10.1	2.3	As above	
	182,947 (open pit)	33,059		5.6			
Golden Mile	9,370 (underground)	3,819	1433	12.6	4.5	As above	
	44,462 (open pit)	6,476		4.5			
Golden West	2,425	969	1594	12.4	20.5	As above	
Rose's Pride	17,683	6,526	1103	11.3	1.8	As above	
Woolgar	24,256	23,143				Proterozoic metasediments	Permo-Carboni
Mt Coolon	280,355	137,253		16.3		Devono-Early Carboni. ignimbrite	
Yandan						Devono-Carboniferous sediments	
Blue Valley						Lower Permian volcanics	

Abbreviations: (1) Minerals: Q, quartz; Ad, adularia; Ser, sericite; Chl, chlorite; Ill, Illite; Cal, calcite; Carb, Carbonate; Lau, laumontite; Flu, fluorite; Py, pyrite; Cpy, chalcopyrite; Sph, sphalerite; Ga, galena; Hes, hessite; Aspy, arsenopyrite; Bio, biotite; Acti, actinolite; Mag, magnetite; Tour, tourmaline; Epi, epidote; Zeo, zeolites. (2) Textures: Crusti, crustiform; Collo, colloform; Chal, chalcedonic

In general, most studied epithermal vein deposits in Queensland formed during the Mid-Late Palaeozoic. They are hosted largely in volcano-sedimentary and/or volcanic rocks of andesitic to rhyolitic composition. These deposits range from individual veins (Woolgar) to bonanza shoots (Mt Coolon) and districts with numerous veins and shoots that are parts of operating mines (Cracow). All the deposits included in this study are of adularia-sericite type (Table 1).

Textural varieties and field occurrences

Four types of adularia in the epithermal veins were recognised (Fig. 1), based mainly on the form and size of the individual crystals observed in thin sections. Very often, aggregates of different types of adularia give distinctive morphologies which are readily identified in handspecimen.

I. Sub-rhombic adularia (Fig. 1A) is common in the epithermal veins, being present at six of the ten locations. Adularia crystals in this group are clearly visible at handspecimen scale, and are commonly orange in colour, 2–4 mm in size and subhedral with more or less rhombic outlines (Fig. 2a). They are usually turbid due to the presence of finely disseminated iron hydroxides (?) and locally have cross-hatched twinning. Minor sericite or calcite alteration may be present in some samples. Typically, sub-rhombic adularia crystals are on the edge of the quartz veins or erratically dispersed within the quartz veins. In the Golden Plateau main lode which has over 250 metres vertical extension, sub-rhombic adularia is commonly found at depth, in association with coarse-grained comb quartz and locally with base-metal sulphides. The same mineralogical association occurs in elsewhere, although the vertical control is not clear due to the shallow exposure depths of these veins. Fluid inclusion study indicates homogenisation temperatures ranging from 254 to 287 °C (20 measurements from quartz and sphalerite which are adjacent to sub-rhombic adularia) in the Dawn vein.

II. Rhombic adularia (Fig. 1B) is widespread and the dominant type of adularia in the epithermal veins, being present in all the studied deposits. It generally shows very fine-grained size (< 0.2 mm), cream to very pale orange colour, and euhedral rhombic forms under the microscope (Fig. 2b). Aggregates of rhombic adularia usually have a moss-like appearance in handspecimen (Fig. 2c). However, the crystals of this type may be indistinguishable in handspecimen because of their extremely small size (< 0.2 mm), particularly if they have poor colour contrast with the adjacent quartz. Rhombic adularia is commonly altered to sericite, and occurs within crustiform (cockade) and colloform bands in association with fine-grained quartz in various textures which are evidence of recrystallisation from a silica gel (Dong et al. 1994). The assays of rock chips and drill cores from Central Extended, Golden Plateau, Mt Coolon and Rose's Pride indicate that 85% of high grade (> 10 g/t Au) samples contain significant amounts of rhombic adularia. Seventy eight measurements from fluid inclusions in calcite which is intergrown with rhombic adularia at Rose's Pride give homogenisation temperatures ranging from 141° to 226 °C. The presence of a silica gel precursor indicated by quartz textures, which are closely associated with rhombic adularia in all deposits, also suggests low formation

Table 1. Continued

Vertical ore ext. (m)	Max. vein width (m)	Mineralogy of vein	Vein texture	Th (°C)	Sal. Wt% NaCl	References
250	5	Q, Ad, Ill, Chl, Hes, Cpy, Py, Sph, Ga	Crustiform Colloform Chalcedonic Recrystallised Comb	180–260	0.0–0.1	Worsley 1994 Brooks 1974 Cracow mine record (unpubl.)
27	1.8	Q, Sph, Ga, Cpy, Py, Ad, Hes	Crustiform Comb	260–285	0.4–0.5	Dong 1993 Brooks 1974
150	2	Q, Ad, Ill, Chl, Cpy Py, Hes, Sph	Crustiform Colloform Chalcedonic Recrystallised	200–270	0.0–0.1	Cracow mine record (unpubl.)
45	1.2	Q, Ill, Py, Ad, Sph, Cpy, Ga	Chalcedonic Crustiform Colloform			Dong 1993 Brooks 1974 Cracow mine record (unpubl.)
16	1.4	Q Ad, Py	Crustiform Comb			Brooks 1974
74	1.2	Q, Cal, Ad, Py, Lau	Replacement	150–210	0.1–0.3	Dong 1993 Brooks 1974
150	2	Q, Chl, Py, Ad. Aspy, Sph, Cpy, Cal, Flu	Crusti, collo. Chal., comb Replacement	180–236	0.0–2.0	Digweed 1991
120	2	Q, Ad, Py, Bio, Acti, Mag, Tour, Epi, Zeo, Carb.	Crusti., collo. Chalcedonic Massive			Wells et al. 1989
80	0.4	Q, Ill, Py, Cal, Ad, Cpy	Crusti., collo. Chalcedonic Replacement			Goulevitch 1992
100	0.5	Q, Ser, Ad, Py	Crusti., collo. Chal., comb Replacement			Dong 1990 (field visit and core inspection)

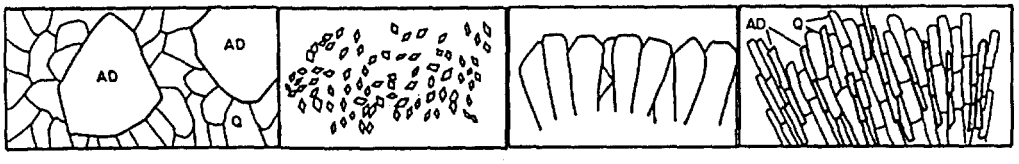

AD: Adularia; Q: Quartz.

	A: Sub-rhombic	B: Rhombic	C: Tabular	D: Pseudo-acicular
Grain size (average)	2 – 4 mm	< 0.2 mm	0.5 – 2 mm	0.1 – 0.5 mm
Common shape of individual grain	Subhedral ± anhedral (rhombic termination)	Euhedral (rhombic)	Euhedral-subhedral (tabular)	Pseudo-acicular
Sericitisation	Rare	Common	Rare	Common
Texture of coexisting quartz	Crystalline Comb ± crustiform	Chalcedonic Microcrystalline Crustiform Colloform	Microcrystalline ± crystalline Crustiform Comb	Chalcedonic Microcrystalline Crustiform Colloform

Fig. 1A–D. The general appearances of adularia varieties in the epithermal veins, Queensland

temperatures (< 220 °C) of rhombic adularia in the epithermal veins (Dong et al. 1994).

III. Tabular adularia (Fig. 1C) is uncommon in the epithermal veins, and is only observed at two locations out of ten. The crystals are generally fine-grained (0.5–2 mm), orange in colour and tabular-shaped (Fig. 2d). They are transparent to translucent with notably less impurities than other types, and are rarely altered. Adularia of this type usually occurs as groups of parallel or subparallel crystals oriented perpendicular to the vein wall in crustiform banded veins, and is associated with fine-grained quartz, chlorite and occasionally with gold. Fluid inclusions from tabular adularia at Central

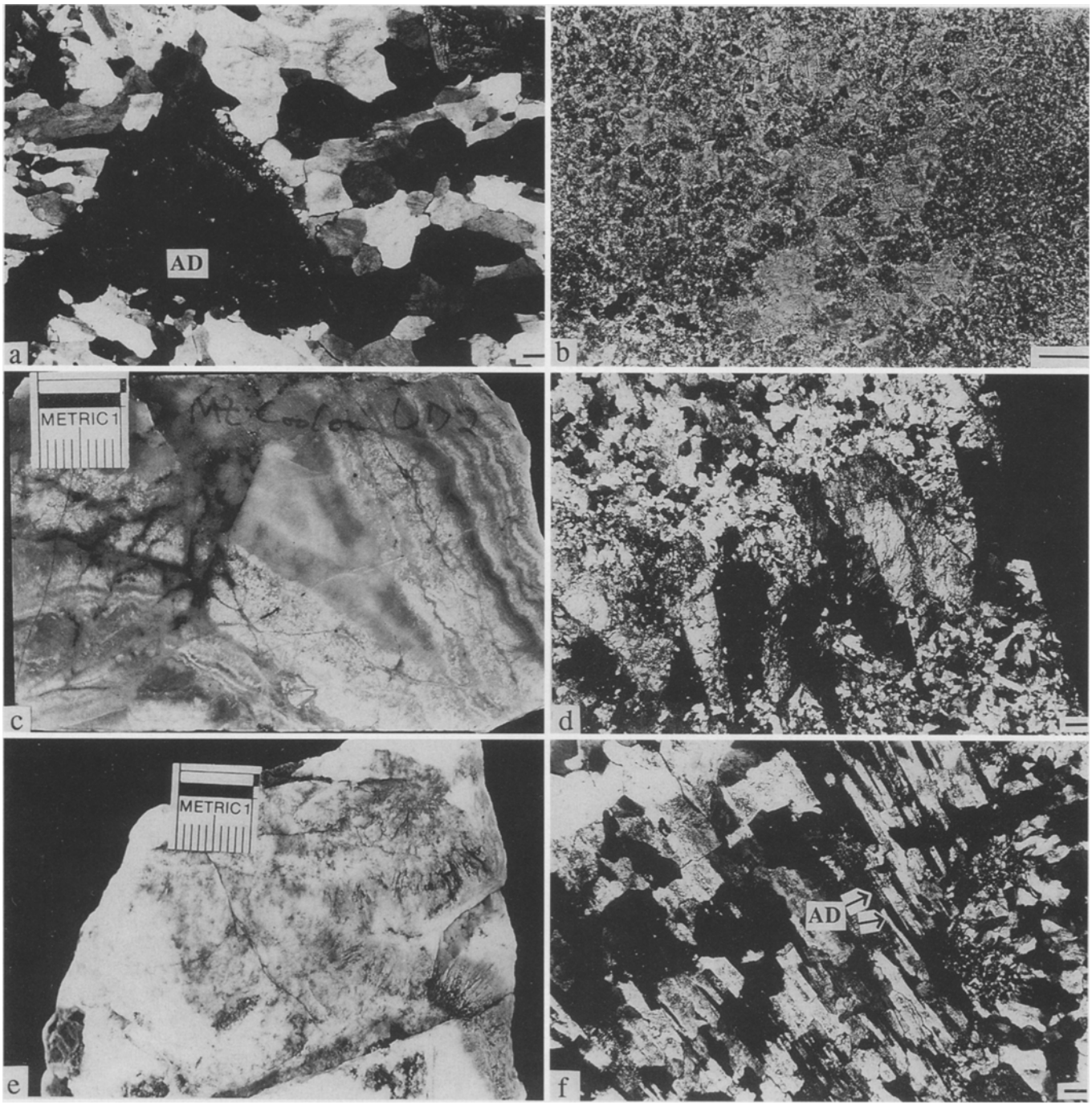

Fig. 2a–f. Adularia textures. **a** The crystals of sub-rhombic adularia are subhedral with more or less rhombic outlines, crossed polars, Golden Plateau lode, Cracow. **b** The crystals of rhombic adularia are very small (< 0.2 mm) and have an euhedral rhombic form, plane polarized light, Mt. Coolon. **c** Aggregates of rhombic adularia, associated with chalcedony, having a moss-like appearance in handspecimen, Mt. Coolon. **d** The crystals of tabular adularia are lath-shaped and contain notably less impurities than other types, crossed polars, Central Extended lode, Cracow, **e** Aggregates of adularia and quartz display a radial-acicular appearance by differences in colour and relief in handspecimen, Blue Valley. **f** Under the microscope, each needle consists of several elongated or ragged adularia grains, crossed polars, Blue Valley. The *scale bars* = 0.2 mm, the metric bars = 1 cm

Extended homogenised at temperatures from 264° to 278 °C (eight measurements).

IV. Pseudo-acicular adularia (Fig. 1D) has been observed in four out of ten locations taken for this study. In handspecimen, aggregates of adularia of this type in association with quartz display a radial-acicular texture indicated by differences in colour and/or relief (Fig. 2e). Under the microscope, each needle actually consists of several small (0.1–0.5 mm) elongate or ragged adularia crystals with a poorly defined crystal habit (Fig. 2f). It has been found that either sheaf-like carbonate or granular carbonate is partially replaced by adularia and quartz along a set of radiating acicular

Table 2. Chemical composition of adularia in the epithermal veins, Queensland

Sample no.	CR12-1	CR12-2	CR12-3	CR01-1	CR01-2	CR01-3	CR26-1	CRX26-2	CR26-3	CR46-1	CR46-2	CR46-3	CR46-4
Type	Sub-rhombic			Pseudo-acicular			Rhombic			Tabular			
SiO_2	64.37	64.51	63.69	64.28	65.52	64.40	64.55	64.35	63.84	65.35	64.18	64.13	65.87
Al_2O_3	18.27	18.07	18.22	18.10	17.39	18.27	18.40	18.10	18.36	17.77	17.92	17.82	17.54
TiO_2	0.00	0.00	0.00	0.00	0.00	0.13	0.00	0.22	0.25	0.08	0.10	0.00	0.00
Cr_2O_3	0.00	0.13	0.00	0.00	0.00	0.23	0.00	0.10	0.00	0.00	0.00	0.12	0.13
FeO	0.00	0.00	0.00	0.00	0.10	0.12	0.00	0.00	0.00	0.00	0.38	0.00	0.22
MnO	0.00	0.00	0.00	0.00	0.00	0.00	0.11	0.00	0.00	0.00	0.00	0.00	0.00
MgO	0.00	0.19	0.00	0.00	0.13	0.00	0.00	0.00	0.00	0.07	0.00	0.00	0.00
CaO	0.00	0.10	0.00	0.00	0.00	0.00	0.00	0.00	0.00	0.00	0.07	0.00	0.00
K_2O	16.94	16.54	16.76	16.90	16.05	16.38	16.42	16.54	16.70	16.11	16.51	16.77	16.13
Na_2O	0.17	0.34	0.14	0.19	0.29	0.26	0.11	0.20	0.22	0.29	0.11	0.32	0.36
Total	99.75	99.88	98.81	99.47	99.48	99.79	99.59	99.51	99.37	99.67	99.27	99.16	100.2
Si	2.99	2.99	2.99	3.00	3.04	2.99	3.00	2.99	2.98	3.02	3.00	3.00	3.03
Al	1.00	0.99	1.01	1.00	0.95	1.00	1.01	0.99	1.01	0.97	0.99	0.98	0.95
Ti	0.00	0.00	0.00	0.00	0.00	0.00	0.00	0.01	0.01	0.00	0.00	0.00	0.00
Cr	0.00	0.00	0.00	0.00	0.00	0.01	0.00	0.00	0.00	0.00	0.00	0.00	0.00
Fe^{2+}	0.00	0.00	0.00	0.00	0.00	0.00	0.00	0.00	0.00	0.00	0.01	0.00	0.01
Mn	0.00	0.00	0.00	0.00	0.00	0.00	0.00	0.00	0.00	0.00	0.00	0.00	0.00
Mg	0.00	0.01	0.00	0.00	0.01	0.00	0.00	0.00	0.00	0.00	0.00	0.00	0.00
Ca	0.00	0.00	0.00	0.00	0.00	0.00	0.00	0.00	0.00	0.00	0.00	0.00	0.00
K	1.01	0.98	1.00	1.01	0.95	0.97	0.97	0.98	0.99	0.95	0.98	1.00	0.95
Na	0.02	0.03	0.01	0.02	0.03	0.02	0.01	0.02	0.02	0.03	0.01	0.03	0.03

Electron microscope analyses were performed on a Jeol Jxa – 840A instrument at James Cook University. ZAF corrections were carried out by Tracor Northern MicroQ software. Atomic contents calculated on the basis of 8 oxygens

fissures, forming a texture identical with pseudo-acicular texture observed in adularia and quartz aggregates. Therefore, pseudo-acicular adularia is considered to be a replacement product, most likely after carbonate (cf. Dong et al. 1994). The adularia of this type is particularly susceptible to sericite or kaolinite alteration, and is associated closely with rhombic adularia, chalcedonic or fine-grained quartz within crustiform (cockade) and colloform bands. It is suggested from the mineral association that the formation temperatures of pseudo-acicular adularia are similar to those of rhombic adularia.

A few samples representative of each adularia type have been checked by microprobe analyses. The results indicate their compositions are close to pure $KAlSi_3O_8$ (Table 2).

Structural state

The key structural units of feldspars are four-membered rings of TO_4 tetrahedra which form double crankshaft-like chains parallel to [100] (Ribbe 1975). The structural states of potassium feldspars can be described on the basis of Al/Si distribution in the non-equivalent tetrahedral sites of these four-membered rings. These are arbitrarily designated as T_1 and T_2 for a monoclinic feldspar, or T_1O, T_1m, T_2O and T_2m for a triclinic feldspar (cf. Ribbe 1984). The Al content of each of the tetrahedral sites (t_i) is commonly derived from unit-cell dimensions of feldspars (e.g., Stewart and Wright 1974; Kroll and Ribbe 1983, 1987). The conventional method of the b–c plot (Stewart and Wright 1974) is used in the present study.

In this study, unit-cell dimensions were determined by least squares refinement of X-ray powder diffraction data using the program LSQ85, an up-dated version of Appleman and Evans (1973). The samples for XRD were ground to fine powder. Quartz was naturally present and was therefore used as an internal standard to calibrate peak positions. Data were collected on a Rigaku-Denki X-ray diffraction system equipped with a Sieray automated retrieval system and a graphic curved crystal post-diffraction monochromater. All samples were scanned from 10–55°2θ in steps of 0.02° at 0.5°/min, using monochromated Cu K$\bar{\alpha}$ (λ = 1.54178 Å). Duplicate determinations of some of the samples showed close agreement, exhibiting a maximum variation in reproducibility of $\pm$ 0.02°2θ.

The X-ray powder diffraction data were treated as both monoclinic and triclinic for refinement. For all samples, only monoclinic refinement gave a proper solution. This is consistent with the X-ray powder-diffraction pattern which shows a single (131) reflection. However, the broadening of the (131) reflection in most of the samples may indicate the presence of subordinate triclinic material which is perhaps not sufficient to affect the overall X-ray powder diffraction pattern (cf. Čerńy and Chapman 1986).

The results are presented in Table 3 and Figure 3. Some rhombic adularia samples which were conspicuously altered to sericite and/or carbonate were also analysed. These samples generally showed higher degrees of Al/Si ordering than unaltered samples of rhombic adularia type (Fig. 3). Considering unaltered adularia only, each group has some specific features in terms of Al/Si ordering:

1. Sub-rhombic adularia is relatively ordered, with $2t_1$ of most samples above 0.84.

2. Rhombic adularia commonly shows medium Al/Si order with $2t_1$ values ranging from 0.64 to 0.80. Exception occurs for two samples from Rose's Pride in which

Table 3. Cell dimensions and $2t_1$ values of adularia in the epithermal veins, Queensland

Sample no.	Location	Descriptions	a (Å)	b (Å)	c (Å)	β (deg)	V (Å^3)	$2t_1$
CR02	Cracow GP	I & comb Qtz in crude bands	8.584	12.981	7.210	115.98	722.23	0.88
CR11	As above	I & comb Qtz & sulphide in bands	8.609	12.996	7.212	116.05	725.02	0.85
CR12	As above	I as blebs in banded comb Qtz veins	8.606	12.993	7.213	116.09	724.38	0.87
CR13	As above	I in comb Qtz veinlet	8.607	13.001	7.212	116.06	724.91	0.84
CR14	As above	III & sulphide & comb Qtz in bands	8.600	13.011	7.197	116.10	723.16	0.72
CR18	As above	I (± Carb. & Seri. altered) in brecciated vein	8.593	12.985	7.213	115.94	723.76	0.89
CR19	As above	I rim on wall rock with comb quartz	8.600	12.985	7.211	116.06	723.37	0.87
CR35	As above	II (heavily carb. & Seri. altered) in delicate bands	8.601	12.993	7.211	116.03	724.07	0.86
CR39	As above	III & comb Qtz & sulphide in bands	8.573	13.001	7.189	115.99	720.77	0.66
CR41	As above	II & fine comb Qtz in crude bands	8.605	13.002	7.194	115.97	723.59	0.72
CR48	As above	I rim on wall rock with comb quartz	8.595	12.978	7.210	115.97	723.01	0.89
CR01	Cracow CE	IV & Chalcedony & fine-gr. Qtz in bands	8.603	12.988	7.203	116.04	723.12	0.82
CR04	As above	III with fine comb Qtz in crude bands	8.599	13.023	7.190	116.11	723.06	0.64
CR07	As above	II & chalcedony & fine gr. Qtz in bands	8.603	13.006	7.199	116.06	723.65	0.75
CR17	As above	II & chalcedony & fine gr. Qtz in bands	8.600	12.997	7.199	115.97	723.37	0.77
CR32	As above	II & chalcedony & fine gr. Qtz & sulphide in bands	8.608	13.000	7.204	116.05	724.20	0.79
CR33	As above	II & fine gr. Qtz & chalcedony in bands	8.585	13.003	7.198	116.05	721.93	0.75
CR40	As above	I with comb Qtz in narrow veinlet	8.606	13.002	7.206	116.07	724.32	0.80
CR45	As above	II (± Seri. altered) with fine-gr. Qtz in bands	8.616	12.990	7.208	116.11	724.37	0.85
CR46	As above	III with fine comb Qtz in bands	8.595	13.012	7.198	116.05	723.15	0.72
CR47	As above	III with fine comb Qtz & fine-gr. Qtz in bands	8.598	13.010	7.192	116.08	722.56	0.68
CR05	Cracow DA	I rim on wall rock with comb Qtz	8.598	12.989	7.214	115.95	724.44	0.89
CR30	As above	II within fine-gr. Qtz	8.604	13.006	7.204	116.12	723.81	0.78
CR06	Cracow GW	I as blebs in banded comb Qtz	8.618	12.987	7.211	116.11	724.72	0.87
CR37	As above	I as blebs in banded comb Qtz	8.613	12.997	7.213	116.11	725.01	0.86
CR38	As above	II & fine comb Qtz in bands	8.593	12.990	7.201	116.09	721.81	0.80
CR03	Cracow GM	II (± Seri. altered) with chalcedony in bands	8.564	12.998	7.204	115.91	721.29	0.80
CR26	As above	II with chalcedony in bands	8.600	13.001	7.188	115.99	722.41	0.68
CR27	As above	II (± Seri. altered) with chalcedony in bands	8.610	13.007	7.207	116.09	724.83	0.80
CR08	Cracow RP	III with fine comb Qtz in bands	8.616	13.011	7.192	116.07	724.17	0.69
CR10	As above	IV & calcite & chalcedony in bands	8.601	12.987	7.207	116.14	722.73	0.85
CR15	As above	II with chalcedony	8.596	12.999	7.191	116.03	722.08	0.71
CR20	As above	II with massive calcite	8.611	12.981	7.203	116.03	723.46	0.83
CR22	As above	II with chalcedony	8.595	12.994	7.193	116.05	721.74	0.74
CR25	As above	II with massive calcite	8.615	12.988	7.210	116.18	723.95	0.87
AD2	Woolgar	II in bladed pseudomorphs	8.613	13.019	7.196	116.01	725.12	0.69
AD5	Mt Coolon	II (± Seri. altered) with chalcedony in bands	8.594	13.004	7.206	116.03	723.62	0.79
AD6	As above	II (brecciated & Seri. altered)	8.588	12.994	7.207	115.94	723.23	0.83
AD7	As above	II (± Seri. altered) with chalcedony in bands	8.584	13.003	7.204	116.02	723.00	0.78
AD8	As above	II (± Seri. altered) with chalcedony in bands	8.586	12.996	7.205	115.97	722.70	0.81
AD11	Yandan	II & chalcedony & sulphide in bands	8.606	13.024	7.191	116.09	723.79	0.64

I, Sub-rhombic; II, Rhombic; III, Tabular; IV, Pseudo-acicular;
GP, Golden Plateau; CE, Central Extended; DA, Dawn; GW, Golden West; GM, Golden Mile; RP, Rose's Pride
The calculated error is ± 0.00n for a, b and c; ± 0.n · 10^{-4} for c*; ± 0.0n for β; ± 0.n for V

adularias coexist with calcite and have ordered structures, with $2t_1$ of 0.83 and 0.87.

3. Tabular adularia is relatively disordered, with $2t_1$ values ranging from 0.64 to 0.72.

4. Only two XRD analyses are available for pseudo-acicular adularia, showing an ordered Al/Si distribution with $2t_1$ of 0.82 and 0.85.

A number of samples show some deviations in the b and c parameters, plotting outside the b–c quadrilateral (Fig. 3). Plotting the lattice-parameter data for a versus b.c in a "strain diagram" of Kroll and Ribbe (1987) (Fig. 4) shows that most of the samples have a negative strain index despite their compositions close to pure $KAlSi_3O_8$ (S.I., in %, = 0 for unstrained alkali feldspars; > 0 for K-rich strained phases and < 0 for Na-rich strained phases, Kroll and Ribbe 1987). This is in a good agreement with investigation by Witt et al. (1985), which indicated that the substitution of H_3O^+ for K, Na or Ca could be responsible to calculate negative strain index for the majority of K-feldspars from the tin-bearing granites in north Queensland. Alternatively, as pointed out by Černý and Chapman (1986), "anomalous" structures are due to a low-triclinicity structural state simulating a monoclinic powder-diffraction pattern by overlap of very closely spaced triclinic peaks (e.g. 131 + $1\bar{3}1$ merging into a single quasi-131 diffraction maximum).

Genetic considerations

The structural state of adularia has been interpreted in two principal ways: (1) metastable crystallisation of

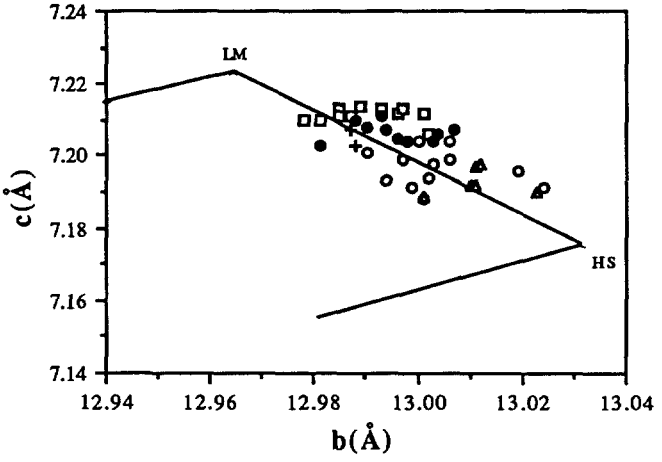

Fig. 3. The b and c cell dimensions of adularia in the epithermal veins, in relation to the low (maximum) microcline (*LM*) and high sanidine (*HS*) data preferred by Stewart and Wright (1974). □ Subrhombic; ○ rhombic; △ tabular; + pseudo-acicular. *Solid symbols* represent adularia with sericite and/or carbonate alteration

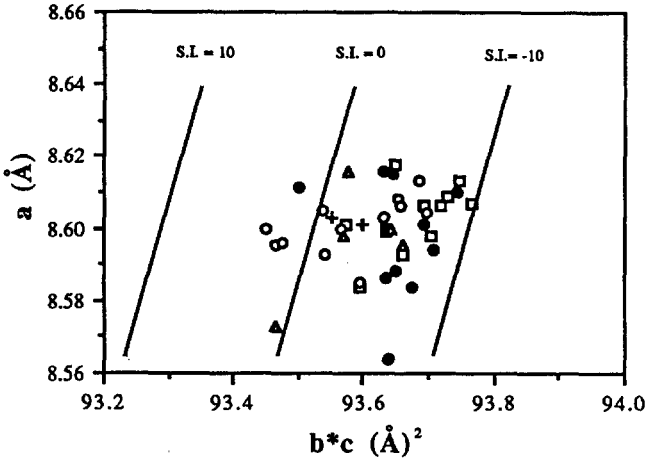

Fig. 4. Plotting the lattice-parameter data a vs. b.c in the diagram of Kroll and Ribbe (1987), contoured for strain index (*S.I.*). Symbols as in Fig. 3

disordered feldspar followed by variable degrees of ordering (transformation), mainly controlled by the post-crystallization thermal regime (Bambauer and Laves 1960; Gubser and Laves 1967); (2) direct crystallisation in the different structural states as observed today, controlled mainly by the process of crystal growth (Steiner 1970; Akizuki and Sunagawa 1978).

At temperatures less than a few hundred °C (e.g. in epithermal environments) ordering in silicates is usually extremely slow in the solid state, even relative to a geological time scale (Carpenter and Putnis 1985). Therefore, the structural state of adularia should be mainly influenced by the process of crystal growth. However, the fact that sericite- and/or carbonate-altered adularias consistently display more ordered structures, suggests that the post-crystallisation thermal regime did affect the structural state of adularia in some way, even at temperatures as low as in epithermal environments.

Yund and Tullis (1980) investigated the effect of trace amounts of water on the kinetics of disordering of albite and microcline experimentally and argued strongly that water is probably the principal factor which controls the structural state of alkali feldspar. This idea was supported by geological evidence that alkali feldspars in high-grade metamorphic rocks tend to be less ordered than those from rocks of lower grade, which formed at lower temperatures, but were also presumably wetter (Guidotti et al. 1973). In addition, within individual feldspar phenocrysts, the more ordered portions of crystals are often observed to be along grain boundaries, cracks, or grain-scale faults where water is likely to have been more abundant (Raase 1976).

It seems likely that adularia shows the same general effects of interaction with water as do other alkali feldspars. Černý and Chapman (1986) examined adularia from various hydrothermal vein deposits and found that highly ordered adularias are typically altered and overgrown by younger minerals.

Combining all information described above, it is reasonable to conclude that the structural state of most unaltered adularia in all epithermal veins is mainly controlled by the process of primary crystal growth, and extensive interaction with later fluids is responsible for advanced ordering in the structure of altered adularia.

The equilibrium order/disorder temperature of K-feldspar is thought to be 450 °C (Bambauer and Bernotat 1982), which is certainly above the crystallisation temperature of adularia in epithermal environments. The presence of adularias with varying degrees of disorder indicates that non-equilibrium conditions prevailed during their crystallisation in epithermal environments. This resulted in the metastable growth of adularias with more or less disordered structures, irrespective of their thermodynamic stability. This agrees with the hypothesis proposed by Chernov and Lewis (1967): "The composition and structure of a crystal formed in a multicomponent system are determined by equilibrium diagram only if the conditions of crystal growth are close to those of equilibrium. If the departure from equilibrium is considerable, both the composition and actual structure of the crystal will depend on the crystallization kinetics."

Carpenter and Putnis (1985) reviewed models of growth for ordered and disordered crystals, and related the degree of supersaturation in a system to the kinetics of crystal growth for various minerals. Each atom has a residence time at the growth point with a finite probability, depending on its attachment energy, of being detached and then replaced. The attachment energy depends on interactions of the arriving atom with preexisting local structure. If the supersaturation is high there is an increased probability that the "wrong" atom would be trapped in place by succeeding atoms, because the growth rate is high (relative to that at lower supersaturation). In other words, the higher the supersaturation the faster the growth rate and the greater the degree of disordering. At a constant supersaturation, lower temperatures reduce the rate of exchange of atoms between the growth surface and supply growth medium and therefore a more ordered crystal structure is in favour. The experimental work by Taroyev et al. (1991) indicates below 400 °C, the $2t_1$ values of K-feldspars increase with falling temperature.

In regards to the structure of the adularias in this study, tabular and rhombic adularias are likely to have grown under condition of high supersaturations in response to rapidly changing conditions. High temperatures, evidenced by the fluid inclusion measurements and the prevalence of the face {010} (Franke et al. 1982), may further increase the growth rate of tabular adularia, resulting in its more disordered structure.

Sub-rhombic adularia is probably formed at low degrees of supersaturation in response to slowly changing conditions. It is not surprising therefore, that coarse comb quartz is commonly associated with sub-rhombic adularia.

High Al/Si ordering in the structure of pseudo-acicular crystals may be attributed to the presence of a carbonate precursor. As indicated by Carpenter and Putnis (1985) and Senderov et al. (1991), the authigenic K-feldspars in carbonate rocks are usually substantially or fully ordered, possibly because of kinetic factors that are not yet understood.

Based on exploration of active geothermal systems, Browne and Ellis (1970), Browne (1978), Henley (1985), and Hedenquist (1990) showed that vein adularia is one of the mineralogical indicators for boiling. Their observation was strongly supported by a number of thermodynamic studies (e.g. Drummond and Ohmoto 1985; Reed and Spycher 1985 and Cathles 1991). Cooling destabilises $Al(OH)_4^-$ and precipitates silicates such as adularia and sericite by the reactions (Reed and Spycher 1985):

$$K^+(aq) + Al(OH)_4^-(aq) + 3SiO_2(aq)$$

$$\rightarrow KAlSi_3O_8(\text{adularia}) + 2H_2O(aq)$$

$$K^+(aq) + 2H^+(aq) + 3Al(OH)_4^-(aq) + 3SiO_2(aq)$$

$$\rightarrow KAl_3Si_3O_{10}(OH)_2(\text{sericite}) + 6H_2O(aq)$$

A higher pH of the boiling fluid fixes adularia, rather than sericite, in accordance with the following reaction (Reed and Spycher 1985):

$$6SiO_2(aq) + KAl_3Si_3O_{10}(OH)_2(\text{sericite}) + 2K^+(aq)$$

$$\rightarrow 3KAlSi_3O_8(\text{adularia}) + 2H^+(aq)$$

When a fluid first boils at deep levels where permeability is low, very little gas can escape from the system. The fluid cools slowly and is only slightly supersaturated with respect to adularia and quartz, causing the precipitation of sub-rhombic adularia, as well as coarse-grained comb quartz. Slowly changing conditions and deep position in vein systems are responsible for ordered Al/Si distribution and general lack of vein sericitic alteration in sub-rhombic adularia's crystals.

As the fluid moves up and encounters an environment of increased permeability which permits effective gas removal, boiling will proceed more violently. Tabular adularia is perhaps an early product of this violent boiling. Relatively high temperatures and rapidly changing conditions are responsible for its disordered structure. Rhombic adularia might also have formed under rapidly changing conditions but at low temperature. This most likely happens when violent boiling is further protracted.

Acicular adularia pseudomorphs, presumably after carbonate, might be formed under more or less the same conditions as rhombic adularia. As boiling is protracted further, the effect of drop in temperature becomes dominant over loss of CO_2. Carbonate, precipitated due to rapid loss of CO_2 during early boiling, will be dissolved and replaced by adularia and quartz.

If cooling and/or mixing of descending acid-condensate fluid with the fluid remaining from boiling continued, the cooled and/or mixed fluid composition could shift back to the K-mica stability field. This perhaps can explain why rhombic adularia and acicular adularia pseudomorphs are commonly altered to sericite.

In epithermal environments, gold is most likely transported as a bisulphide complex (Berger and Henley 1989). As pointed by Drummond and Ohmoto (1985), boiling has two competing effects upon the solubility of gold: increasing pH, due to loss of CO_2 from the solution, increases the solubility of gold within the pH range wherein H_2S dominates over HS^-, whereas loss of H_2S decreases gold solubility according to the reaction (Drummond and Ohmoto 1985):

$$8Au^\circ + 15H_2S(aq) + SO_4^{-2}(aq) \rightleftharpoons 8Au(HS)_2^-(aq)$$

$$+ 4H_2O(aq) + 6H^+(aq)$$

H_2S is more soluble than CO_2, therefore when a fluid first boils H_2S loss is proportionally less than CO_2, the net effect of the boiling is slight increase of gold solubility. It is only when boiling is protracted that the effect of H_2S loss becomes dominant over pH change in determining gold stability and significant amounts of gold will precipitate. Consequently, it is not surprising that adularia of rhombic and pseudo-acicular types, formed when boiling is protracted, is associated closely with high grade ore.

Conclusions

A consistent pattern of the textural type and structural state of adularia in epithermal veins from Queensland suggests that different textural types are formed in response to different depositional conditions. Sub-rhombic adularia has a relatively ordered structure ($2t_1 > 0.84$), reflecting slow crystallisation conditions. In contrast, rhombic and tabular adularia crystals are characterised by a higher Al/Si disordered structure with $2t_1$ commonly ranging from 0.64 to 0.80, implying rapid crystallisation conditions. Pseudo-acicular adularia texture has been inferred as a pseudomorphous replacement of carbonate, and high Al/Si ordering in the structure of adularia of this type may be attributed to the presence of carbonate precursor. Both field evidence and deduced formation conditions suggest that the presence of rhombic and pseudo-acicular adularia is a good indicator of gold mineralisation.

Acknowledgements. This paper represents part of a completed Ph.D. thesis by the senior author. Sincere thanks are due to Drs. Chris Cuff, Subhash Jaireth and Myles Worsley for their valuable comments and support. Two Mineralium Deposita reviewers are sincerely thanked for their constructive comments. Funding for the project was provided by the Australian Mineral Industries Research Association (AMIRA), who and sponsor companies are gratefully acknowledged.

References

Akizuki, M., Sunagawa, I. (1978) Study of the sector structure in adularia by means of optical microscopy, infra-red absorption, and electron microscopy. Mineral. Mag. 42:453–462

Appleman, D.E., Evans, H.T., Jr. (1973) Job 9214: indexing and least-squares refinement of powder diffraction data: U.S. Geol. Surv., Comp. Contr. 20 (NTIS Document PB2-16188)

Bambauer, H.U., Bernotat, W.H. (1982) The microcline/sanidine transformation isograd in metamorphic regions. I. Composition and structural state of alkali feldspars from granitoid rocks of two N-S traverses across the Aar Massif and Gotthard, Swiss Als. Schweiz. Min. Petr. Mitt. 62:185–230

Bambauer, H.U., Laves, F. (1960) Zum Adularproblem. Schweiz. Min. Petr. Mitt. 40:177–205

Berger, B.R., Henley, R.W. (1989) Advances in understanding of epithermal gold-silver deposits, with special reference to the Western United States. Econ. Geol. 84:405–423

Brooks, J.H. (1974) Departmental diamond drilling programme – Cracow Goldfield. Geol. Surv. Old. Report, No. 81, 38 p

Browne, P.R.L. (1978) Hydrothermal alteration in active geothermal fields. Ann. Rev. Earth Planet. Sci. 6:229–250

Browne, P.R.L., Ellis, A.J. (1970) The Ohaki-Broadlands hydrothermal area, New Zealand: mineralogy and related geochemistry. Am. J. Sci. 269:97–131

Buchanan, L.J. (1981) Precious metal deposits associated with volcanic environments in the Southwest. In: Dickinson, W.R. (eds.) Relations of tectonics to ore deposits in the South Cordillera. Arizona Geological Society Digest 14:237–262

Carpenter, M.A., Putnis, A. (1985) Cation order and disorder during crystal growth: some implications for natural mineral assemblage. In: Thompson, A.B., Rubie, D.C. (eds.) Metamorphic reactions: kinetics, textures and deformation: Springer, Berlin Heidelberg New York, pp. 1–26

Cathles, L.M. (1991) The importance of vein selvaging in controlling the intensity and character of subsurface alteration in hydrothermal systems. Econ. Geol. 86:466–471

Černý, P., Chapman, R (1984) Paragenesis, chemistry and structural state of adularia from granitic pegmatites. Bull. Mineral. 107:369–384

Černý, P., Chapman, R. (1986) Adularia from hydrothermal vein deposits: extremes in structural state. Can. Mineral. 24:717–728

Chernov, A.A., Lewis, J. (1967) Computer model of crystallization of binary systems: kinetic phase transitions. J. Phys. Chem. Solids 28:2185–2198

Colville, A.A., Ribbe, P.H. (1968) The crystal structure of an adularia and a refinement of the structure of orthoclase. Am. Mineral. 53:25–37

Digweed, J.M. (1991) The geology and zoning of epithermal gold-quartz veins at Woolgar, North Queensland. Unpubl. M.Sc. thesis, James Cook University, Australia, 173 p

Dimitriadis, S., Soldatos, K. (1978) Optical and structural properties of adularia from Xanthi and Ouranoupolis, Greece, and their interpretation. Neues Jahrb. Mineral. Abh. 133:88–105

Dong, G. (1993) Textures of quartz and adularia, and their zoning in epithermal veins, Queensland. Unpubl. Ph.D. thesis, James Cook University, Australia, 233 p

Dong, G., Morrison, G.W., Jaireth, S. (1994) Quartz textures in epithermal veins, Queensland – classification, origin and implication. Econ. Geol. (in press)

Drummond, S.E., Ohmoto, H. (1985) Chemical evolution and mineral deposition in boiling hydrothermal systems. Econ. Geol. 80:126–147

Franke, W., Brettschneider, E., Ghobarkar, H., Grothe, C.H., Zarei, M. (1982) The morphology of hydrothermal growth alkali feldspars. In: Minceva-Stefanova, J. (ed.) Morphology and phase equilibria of minerals. Proceedings of the 13th General Meeting of International Mineralogical Association, Varna, Sept. 1982. Publishing House of the Bulgarian Academy of Sciences, Sofia, pp. 153–161

Goulevitch, J. (1992) Aspects of epithermal gold mineralisation at East Hill, Yandan, Queensland, Unpubl. M.Sc. thesis, James Cook University, Australia, 186 p

Gubser, R., Laves, F. (1967) On X-ray properties of "adularia", [K, Na] $AlSi_3O_8$. Schweiz. Mineral. Petr. Mitt. 47:177–188

Guidotti, C.V., Herd, H.H., Tuttle, C.L. (1973) Composition and structural state of K-feldspars from K-feldspar plus sillimanite grade rocks in northwestern Maine. Am. Mineral. 58:705–716

Heald, P., Foley, N.K., Hayba, D.O. (1987) Comparative anatomy of volcanic-hosted epithermal deposits: acid-sulfate and adularia-sericite types. Econ. Geol. 82:1–26

Hedenquist, J.W. (1990) The thermal and geochemical structure of the Broadlands-Ohaaki geothermal system. Geothermics 19:151–185

Henley, R.W. (1985) The geothermal framework of epithermal deposits. In: Berger, B.R., Bethke, P.M. (eds.) Geology and geochemistry of epithermal systems. Rev. Econ. Geol. 2:1–24

Kroll, H., Ribbe, P.H. (1983) Lattice parameters, composition and Al, Si order in alkali feldspars. Reviews in Mineralogy, Vol. 2, 2nd edn. Mineral. Soc. Am., Blacksburg, Virginia, pp. 57–99

Kroll, H., Ribbe, P.H. (1987) Determining (Al, Si) distribution and strain in alkali feldspars using lattice parameters and diffraction-peak positions. A review. Am. Mineral. 72:491–506

Raase, P. (1976) The potassic feldspar in metamorphic rocks from the western Hohe Tauern area, eastern Alps. Geol. Rundsch. 65:422–436

Reed, M.H., Spycher, N.F. (1985) Boiling, cooling, and oxidation in epithermal system: a numerical modelling approach. In: Berger, B.R., Bethke, P.M. (eds.) Geology and geochemistry of epithermal systems. Rev. Econ. Geol. 2:249–272

Ribbe, P.H. (ed.) (1975) Feldspar mineralogy: reviews in mineralogy. Mineral. Soc. Am. Short Course Notes, Vol. 2. Blacksburg, Virginia, 289 p

Ribbe, P.H. (1984) The average structures of feldspars. In: Brown, W.L. (eds.) Feldspars and feldspathoids – structures, properties and occurrences. Reidel, Dordrecht, Holland, pp. 1–94

Senderov, E.E., Hearn, P.P., Jr., Kuznetsova, T., Tobelko, K.I. (1991) The structural state of secondary K-feldspars in relation to the conditions of their formation. Geochem. Int. 28: No. 9, 22–35

Smith, J.V. (1974) Feldspar minerals, I. Crystal structure and physical properties. Springer, Berlin Heidelberg New York, 627 p

Steiner, A. (1970) Genesis of hydrothermal K-feldspar (adularia) in an active geothermal environment at Wairakei, New Zealand, Mineral. Mag. 37:916–922

Stewart, D.B., Wright, T.L. (1974) Al/Si order and symmetry of natural alkali feldspars, and the relationship of strained cell parameters to bulk composition. Soc. Franc. Mineral. Crist. Bull. 97:356–377

Taroyev, V.K., Tauson, V.L., Abramouich, M.G. (1991) Laboratory data on the initial state of ordered potash feldspar. Geochim. Int. 28: No. 10, 120–123

Wells, K., Murray, A.M., Cunneen, R.D. (1989) The geology and exploration of Mt Coolon gold deposit: In: N.Q. Gold'89 – Proceedings, The Aust. I.M.M., April 1989, Townsville, Australia, pp. 111–114

Witt, K.W., Chitrakar, R., Pollard, P.J., Johnston, C., Cuff, C., Taylor, R.G. (1985) Mineralogical and crystallochemical studies on feldspars from granites associated with mineralisation in the Herberton Tinfield North Queensland, Australia. First Symposium and Workshop on Tin Tungsten Granites in Southeast Asia and the Western Pacific, April 1985, Thailand

Worsley, M. (1994) Golden Plateau mine, Cracow, Central Queensland: geology, ore shoot controls and origin of gold mineralisation. Unpubl. Ph.D. thesis, James Cook University, Australia, 298 p

Yund, A., Tullis, J. (1980) The effect of water, pressure, and strain on Al/Si order-disorder kinetics in feldspar. Contrib. Mineral. Petrol. 72:297–302

Editorial handling: T. Seward